Available online at www.sciencedirect.com
SCIENCE DIRECT®
Journal of Molecular Catalysis A: Chemical 223 (2004) 295–304
JOURNAL OF MOLECULAR CATALYSIS A: CHEMICAL
www.elsevier.com/locate/molcata

Stabilization of nanosized titania-anatase for high temperature catalytic applications

Benjaram M. Reddy*, Ibram Ganesh, Ataullah Khan

Inorganic and Physical Chemistry Division, Indian Institute of Chemical Technology, Hyderabad 500007, India

Received 10 May 2003; received in revised form 27 January 2004; accepted 1 February 2004
Available online 11 September 2004

Abstract

M_2O_3–TiO_2 (M = Ga, In and La) composite oxides were prepared by a co-precipitation method with in situ generated ammonium hydroxide and were impregnated with 12 wt.% V_2O_5. The M_2O_3-TiO_2 and V_2O_5/M_2O_3-TiO_2 (M = Ga, In and La) samples were subjected to thermal treatments from 773 to 1073 K and were investigated by X-ray diffraction, FT-infrared, and BET surface area methods to establish the effects of vanadia loading and thermal treatments on the surface structure of the dispersed vanadium oxide species and temperature stability of these catalysts. Characterization results suggest that the co-precipitated M_2O_3–TiO_2 composite oxides are in X-ray amorphous state and exhibit reasonably high specific surface area at 773 K calcination. The M_2O_3-TiO_2 mixed oxide supports also accommodate a monolayer equivalent of V_2O_5 (12 wt.%) in a highly dispersed state. The V_2O_5/M_2O_3-TiO_2 catalysts are thermally stable up to 873–973 K calcination temperature. When subjected to thermal treatments beyond 873–973 K, the dispersed vanadium oxide selectively interacts with In_2O_3 or La_2O_3 portions of the respective mixed oxides and forms $InVO_4$ or $LaVO_4$ compounds. The remaining TiO_2 appears in the form of anatase or rutile phase. In the case of V_2O_5/Ga_2O_3-TiO_2 sample, no such surface vanadate compound formation was observed. All samples were evaluated for one step synthesis of 2,6-dimethylphenol from cyclohexanone and methanol mixtures in the vapour phase at normal atmospheric pressure. The 12% V_2O_5/La_2O_3-TiO_2 catalyst exhibited good conversion and product selectivity among various samples investigated.

Keywords: Titanium oxide; Gallium oxide; Lanthanum oxide; Indium oxide; Mixed oxides; V_2O_5; Dispersion; Acid–base properties; Redox properties; Cyclohexanone; Methanol; 2,6-Dimethylphenol

1. Introduction

Titanium oxide is a widely used material in the production of pigments, catalysts, photocatalysts, solar cells, optical thin film filters, etc. Titania, as a catalyst, exhibits a number of attractive characteristics such as chemical stability, non-toxicity, low cost and the highest oxidation rate of the many active metal oxides investigated. The unique physicochemical properties of TiO_2 also offer an exciting spectrum of applications having the additional advantage of being biocompatible, environmentally friendly, and readily available material [1–3]. The vanadium-titanium oxides are the basic components of industrial catalysts for selective catalytic reduction (SCR) of nitrogen oxides, selective oxidation of various hydrocarbons, and ammoxidation of N-heteroaromatic compounds [4–7]. In particular, titania-anatase has been extensively used for several photocatalytic reactions for the elimination of many organic pollutants from waste-waters [8,9]. Titania-based catalysts were also employed for HCN and COS hydrolysis, olefin epoxidation [10], and precious metal (Pt, Rh or Ru) or Ni impregnated titania for Fischer–Tropsch synthesis [11]. The TiO_2 has also been used as an oxygen sensor to monitor automobile engine performance [1]. Numerous other reactions such as oxidation of H_2S to SO_2, dehydration of alcohols, isomerization, and alkylation have also been studied by employing TiO_2 catalysts [1,2,12]. However, there are some disadvantages associated with TiO_2, which include low specific surface area, poor thermal stability, poor mechanical strength, and lack of

* Corresponding author. Fax: +91 40 2716 0921.
E-mail address: bmreddy@iict.res.in (B.M. Reddy).

1381-1169/$ – see front matter © 2004 Elsevier B.V. All rights reserved.
doi:10.1016/j.molcata.2004.02.031

abrasion resistance. Sintering of TiO_2 results from several processes, one of them is phase transformation from anatase to thermodynamically stable rutile form. Therefore, much effort has been made in recent years to overcome this problem by making new catalyst formulations, which can enhance the thermal (textural) stability of TiO_2 (A) without loosing its unique physicochemical properties. Formation of compounds or solid solutions with many rare earth elements and other transition metals has been attempted in order to improve the thermal stability, mechanical strength and specific surface area of titania-anatase [1,13–24].

Recently, Ga-based zeolites are being extensively employed for light paraffin aromatization in Cyclar process [25]. Also gallium-based oxides find utility in dehydrocyclodimerization of isobutene/isobutane into xylenes [26]. Kikuchi and co-workers [27] introduced indium into various zeolites and reported high activity and selectivity for NO_x reduction. Lanthanum-based composite oxides are employed for various purposes, such as oxidation of chlorodifluoromethane, oxidative coupling of methane, automobile catalytic converter, ceramic membrane top layer, and adsorbent [28–32]. In view of their significance, a comprehensive investigation was undertaken by the authors to fully understand the evolution and physicochemical characteristics of M_2O_3-TiO_2 (M = Ga, In and La) complex oxide systems. The primary objective of this study was to provide basic insights into the structure of M_2O_3-TiO_2 and V_2O_5/M_2O_3-TiO_2 catalysts, shedding light on the influence of thermal treatments, oxide loading, and preparation method on both thermal stability and physicochemical characteristics of these materials. In this study, Ga, In, and La incorporated titanium-based composite oxides were prepared by a homogeneous co-precipitation method with in situ generated ammonium hydroxide and were impregnated with a monolayer equivalent of vanadium pentoxide. The M_2O_3-TiO_2 mixed oxides and V_2O_5/M_2O_3-TiO_2 catalysts were subjected to thermal treatments from 773 to 1073 K and were investigated by TGA–DTA, XRD, FTIR, and BET surface area methods. The catalytic properties of these oxides were evaluated for one step synthesis of 2,6-dimethylphenol from methanol and cyclohexanone mixtures in the vapor phase.

2. Experimental methods

2.1. Catalyst preparation

All composite oxides studied in this investigation were prepared by a homogeneous co-precipitation method using urea as hydrolyzing agent. An appropriate amount of $TiCl_4$ (Fluka, AR grade) was initially digested in cold concentrated HCl and then diluted with doubly distilled water. To this aqueous solution the required quantity of $Ga(NO_3)_3$ (Aldrich, GR grade) or $La(NO_3)_3$ (Aldrich, GR grade) or $InCl_3$ (Aldrich, GR grade), dissolved separately in deionized water, was added. An excess amount of urea solid (Loba Chemie, GR grade) was also added to this mixture solution for better control of pH and heated to 368 K with vigorous stirring. After about 6 h of heating a white precipitate was gradually formed in the solution as the urea decomposition progressed to a certain extent. The precipitate was heated for 6 h more to facilitate aging. The precipitate thus obtained was thoroughly washed with deionized water until no chloride ions could be detected with $AgNO_3$ in the filtrate. The obtained cake was oven dried at 393 K for 16 h and then calcined at 773 K for 5 h. Some portions of the finished support were further calcined at 873, 973 and 1073 K for 5 h. To impregnate V_2O_5 (12 wt.%), the required amount of ammonium metavanadate was dissolved in 1 M oxalic acid solution, and the finely powdered calcined (773 K) support material was added to this solution. Excess water was evaporated on a water bath with continuous stirring. The resultant solid was oven dried at 383 K for 12 h and calcined at 773 K for 5 h in a flow of oxygen. Some portions of the finished catalyst were once again heated at 873, 973 and 1073 K for 5 h in air atmosphere. The rate of heating was always maintained at 10 K min^{-1}.

2.2. Catalyst characterization

The X-ray powder diffraction patterns have been recorded on a Siemens D-5000 diffractometer by using Cu Kα radiation source and Scintillation Counter detector. The XRD phases present in the samples were identified with the help of ASTM Powder Data Files. The crystallite size of TiO_2 anatase and rutile were estimated with the help of Debye–Scherrer equation using the XRD data of anatase (0 1 0) and rutile (1 1 0) reflections [33]. The FTIR spectra were recorded on a Nicolet 740 FTIR spectrometer at ambient conditions, using KBr disks, with a normal resolution of 4 cm^{-1} and averaging 100 spectra. A conventional all glass volumetric high vacuum (up to 1×10^{-6} Torr) system was used for BET surface area measurements. The BET surface area was measured by nitrogen physisorption at liquid nitrogen temperature (77 K) by taking 0.162 nm^2 as the area of cross section of N_2 molecule.

2.3. Catalyst evaluation

The one step synthesis of 2,6-dimethylphenol from methanol and cyclohexanone was investigated in vapour phase under normal atmospheric pressure, in a down flow fixed bed differential micro-reactor, at different temperatures. In a typical experiment ca. 0.5–2.0 g of catalyst sample was secured between two plugs of Pyrex glass wool inside the glass reactor (Pyrex glass tube i.d. 0.8 cm) and above the catalyst bed filled with glass chips in order to act as preheating zone. The reactor was placed vertically inside a tubular furnace, which can be heated electrically. The reactor temperature was monitored by a thermocouple with its tip located near the catalyst bed and connected to a temperature indicator–controller. The catalyst was heated in a flow of air at 723 K for 5 h, prior to the reaction. The mixture of methanol and cyclohexanone was fed from a motorized syringe pump

(Perfusor Secura FT, Germany) into the vaporizer where it was allowed to mix uniformly with air or nitrogen before entering the preheating zone of the reactor. The liquid products collected through spiral condensers in ice cooled freezing traps were analyzed by a gas chromatograph. The liquid products were quantified by FID with a 10% Carbowax 20M (length, 2 m) column. The main products observed were 2,6-dimethylphenol, 2,6-dimethylcyclohexanone, 2-methylcyclohexanone, 1-methoxycyclohexene and some unidentified products. At higher temperatures some small amounts of CO and CO_2 were also noticed. The activity data were collected under steady-state conditions. The conversion, selectivity, and yield were calculated as per the procedure described elsewhere [34].

3. Results and discussion

The BET surface areas of various M_2O_3-TiO_2 (M = Ga, In and La) composite oxides and their corresponding vanadia-impregnated samples are shown in Table 1. Surface monolayer coverage of vanadia on various oxide supports could be estimated from structural calculations [16]. The monolayer surface coverage is defined as the maximum amount of amorphous or two-dimensional vanadium oxide over-layer in contact with the surface of the oxide support. From V–O bond lengths of crystalline V_2O_5 the monolayer surface coverage is estimated to be 0.145 wt.% V_2O_5/m^2 of the support. However, in reality the maximum amount of vanadium oxide that can be formed as two-dimensional vanadium oxide over-layer, i.e. monolayer coverage depends not only on the support surface area but also on the concentration of reactive surface hydroxyl groups apart from other preparative variables [6,13,35]. In view of these reasons a nominal 12 wt.% V_2O_5 loading was selected in the present investigation. As can be observed from Table 1, the surface area of vanadia-impregnated samples is lower than that of pure supports. The decrease in the specific surface area after impregnating with V_2O_5 could be due to various factors such as penetration of the dispersed vanadium oxide into the pores of the support thereby narrowing its pore diameter, blocking some of the pores, and solid-state reactions between the dispersed vanadium oxide and the support [6,21,22]. The XRD measurements described in the subsequent paragraphs strongly support the latter possibility. From the above discussion it can be inferred that the pure supports are quite thermally stable when compared to that of vanadia-impregnated samples.

The various M_2O_3-TiO_2 and 12% V_2O_5/M_2O_3-TiO_2 samples calcined from 773 to 1073 K were characterized by X-ray powder diffraction technique. The XRD patterns of M_2O_3-TiO_2 samples calcined at 773 and 1073 K are depicted in Fig. 1. As can be observed from Fig. 1, all supports calcined at 773 K exhibit broad diffraction patterns due to poor crystalline state. The XRD patterns of Ga_2O_3-TiO_2 support reveal the presence of lines due to TiO_2-anatase (JCPDS Files no. 21-1272) and α-Ga_2O_3 (JCPDS File no. 6-503) phases, respectively. The intensity of lines pertaining to these phases increased with increasing calcination temperature due to better crystallization at higher calcination temperatures. There is no evidence about the formation of any compounds between gallium and titanium oxides in the present study. However, Rozdin et al. reported the formation of three different gallium titanates: metatitanate ($Ga_2O_3{\cdot}TiO_2$), dititanate ($Ga_2O_3{\cdot}2TiO_2$) and tritanate ($Ga_2O_3{\cdot}3TiO_2$) designated as δ phase [36,37]. The non-appearance of these compounds could be attributed due to a different preparative analogy and thermal treatment procedure adopted in the present study to make these composite oxides. An interesting observation to be noted from Fig. 1 is that even up to 1073 K calcination there is no evidence about the formation of TiO_2-rutile phase, which is usually observed in impurity free TiO_2 samples at 873 K and above calcination temperatures. The XRD patterns of In_2O_3-TiO_2 support calcined at 773 K exhibit broad diffraction lines due to TiO_2 (A). As the calcination temperature increases some additional lines are observed at d = 2.92, 1.79 and 2.53 Å due to crystalline In_2O_3 (JCPDS Files no. 6-416). Here too, the intensity of the lines due to TiO_2 (A) and In_2O_3 increased with increasing calcination temperature. Even at 1073 K, formation of no new compounds between indium and titanium oxides were observed. The

Table 1
BET surface area and TiO_2 crystallite size (D_{XRD}) measurements of M_2O_3-TiO_2 and V_2O_5/M_2O_3-TiO_2 catalysts (M = Ga, In and La) calcined at different temperatures

Calcination temperature (K)	Ga_2O_3-TiO_2 (1:5)		In_2O_3-TiO_2 (1:13)		La_2O_3-TiO_2 (1:5)	
	BET SA (m^2g^{-1})	D_{XRD} (nm)	BET SA (m^2g^{-1})	D_{XRD} (nm)	BET SA (m^2g^{-1})	D_{XRD} (nm)
773	122	6.1 (A)	132	9.4 (A)	123	0.4 (A)
873	96	7.1 (A)	98	10.4 (A)	84	5.6 (A)
973	73	12.9 (A)	65	11.0 (A)	77	6.8 (A)
1073	51	19.6 (A)	33	26.7 (A)	38	9.1 (A)
	V_2O_5/Ga_2O_3-TiO_2		V_2O_5/In_2O_3-TiO_2		V_2O_5/La_2O_3-TiO_2	
773	96	8.7 (A)	62	11.5 (A)	64	9.8 (A)
873	77	21.2 (R)	24	25.6 (A)	62	11.2 (A)
973	22	28.7 (R)	18	28.2 (R)	25	14.4 (A)
1073	7	19.6 (R)	1	25.4 (R)	15	14.0 (A)

The TiO_2 anatase (1 0 1) and rutile (1 1 0) reflections were used for crystallite size measurements.

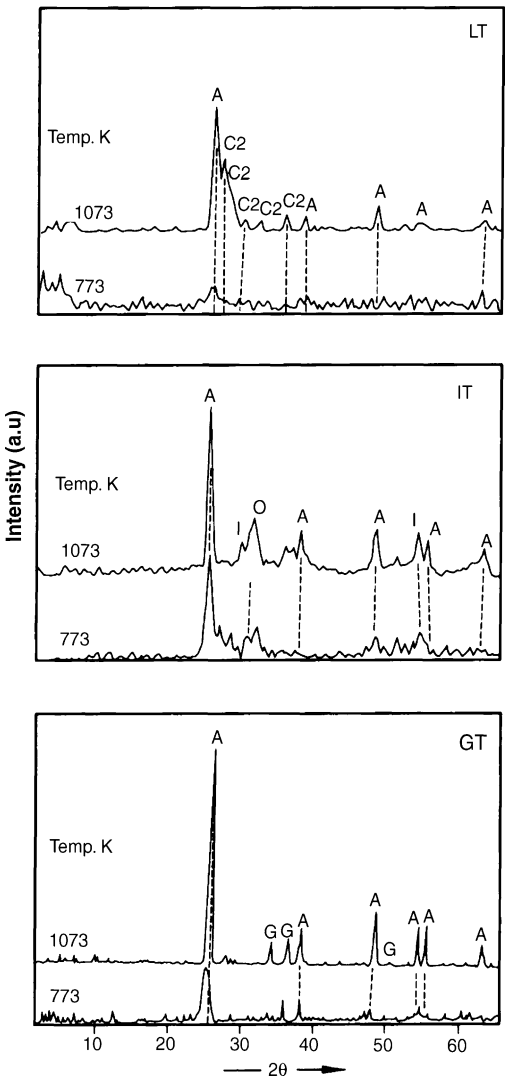

Fig. 1. X-ray powder diffraction patterns of various M_2O_3-TiO_2 (M = Ga^{3+}, In^{3+} and La^{3+}) binary oxides calcined at 773 and 1073 K temperatures: (A) lines due to TiO_2 anatase; (G) lines due to α-Ga_2O_3; (I) lines due to In_2O_3; (C1) lines due to $La_2Ti_2O_7$; (C2) lines due to $La_4Ti_9O_{24}$.

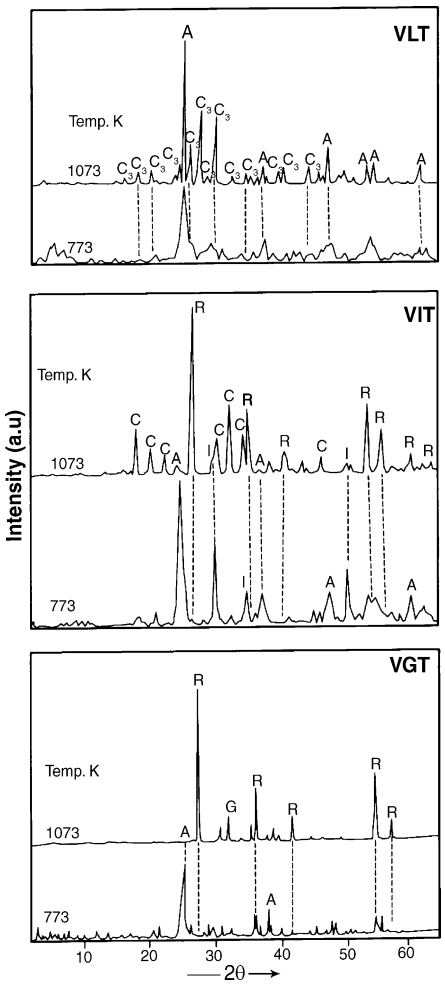

Fig. 2. X-ray powder diffraction patterns of various V_2O_5/M_2O_3-TiO_2 (M = Ga^{3+}, In^{3+} and La^{3+}) catalysts calcined at 773 and 1073 K temperatures: (A) lines due to TiO_2 anatase; (G) lines due to α-Ga_2O_3; (I) lines due to In_2O_3; (C) lines due to $InVO_4$; (C3) lines due to $LaVO_4$.

X-ray diffraction profiles of La_2O_3-TiO_2 support calcined at 773 K reveal broad background diffraction patterns due to poorly crystalline TiO_2 (A) phase. As calcination temperature increases additional lines at d = 2.99, 2.71 and 3.22 Å were observed, which could be attributed due to the formation of $La_2Ti_2O_7$ (JCPDS Files no. 28-517) compound. On further increase of calcination temperature (973–1073 K) an additional set of lines appeared at d = 3.36, 3.28 and 2.54 Å due to $La_4Ti_9O_{24}$ (JCPDS Files no. 15-324) compound at the expense of $La_2Ti_2O_7$. Similar observations were reported by Gopalan and Lin [38]. As mentioned earlier, in this case also there was no evidence about the presence of TiO_2 (R) phase. A similar non-appearance of TiO_2 (R) phase in the case of RE_2O_3-TiO_2 (where RE = La, Y and Ce) mixed oxides was reported and attributed to the stabilization of anatase phase by the surrounding rare earth oxides through the formation of Ti–O–RE bonds by Lin and Yu [39]. Anderson and Bard [40], offered a similar explanation for TiO_2-SiO_2 catalyst system. On those lines a similar analogy can be extended to the present catalyst systems for non-appearance of TiO_2 (R) phase.

The XRD patterns of the V_2O_5/M_2O_3-TiO_2 (M = Ga, In and La) samples calcined at 773 and 1073 K are represented in Fig. 2. As can be noted from Fig. 2, the XRD profile of 12% V_2O_5/Ga_2O_3-TiO_2 sample calcined at 773 K exhibits lines due to poorly crystalline TiO_2 (A) and α-Ga_2O_3 (JCPDS File no. 6-503) phases. As the calcination temperature increases, additional lines at d = 2.816, 2.547 and 2.924 Å due to β-Ga_2O_3 (JCPDS File no. 11-370) and TiO_2 (R) were observed. Interestingly, the transformation of α-Ga_2O_3 → β-Ga_2O_3 and anatase → rutile is complete at 873 K and above calcination temperatures. The intensity of the lines pertaining to the latter phases increased with increasing calcination temperature. There are no lines either due to crystalline vanadia or to a compound between vanadia and mixed oxide

components. Probably during the anatase to rutile phase transformation some of the dispersed vanadia must have reduced and got incorporated into the TiO_2 lattice thereby forming $V_xTi_{(1-x)}O_2$ rutile solid solution, a well documented fact in the literature [2,6]. The XRD profiles of 12% V_2O_5/In_2O_3-TiO_2 sample calcined at 773 K exhibit lines due to TiO_2 (A) and In_2O_3 (JCPDS Files no. 6-416). As the calcination temperature increases, additional set of lines at d = 2.70, 2.53 and 1.51 Å could be seen due to γ-$InVO_4$ (JCPDS Files no. 31-605) compound formation. At 973 K, a partial transformation of anatase to rutile is noted and complete rutile phase is observed at 1073 K. The XRD profiles of 12% V_2O_5/La_2O_3-TiO_2 sample calcined at 773 K (Fig. 2) reveal lines due to TiO_2 (A) and poorly crystalline $LaVO_4$ (JCPDS Files no. 25-427) phase. The intensity of these lines increased with increasing calcination temperature. Very interestingly, there is no evidence for the formation of TiO_2 (R) or crystalline vanadia phase. Retention of TiO_2 (A) beyond 1073 K even in the presence of monolayer equivalent of vanadia is highly beneficial for several thermal/photo catalytic applications and also in the area of material science. It is evident from the present study that addition of lanthanum oxide to TiO_2 (A) retards the thermodynamically feasible anatase to rutile phase transformation.

The formation of MVO_4 (M = In and La) phase can be explained by taking into account the charge to radius ratio of the mixed oxides as envisaged by Bond and Tahir [6]. Formation of surface compounds or uni-dimensional layers of vanadium oxide on various oxide supports has been related to the ratio of the charge of the support cation to the sum of radii of cation and oxide ion (q/r). Normally, lower q/r ratios favor surface compound formation. The q/r ratios for vanadia-M (M = In and La) combinations are lower than the ratios for vanadia-Ti combination, as the ionic radii of In^{3+} and La^{3+} (0.81 and 1.06 Å, respectively) are greater than Ti^{4+} (0.68 Å). Therefore, the dispersed vanadium oxide is expected to interact selectively with the india or lanthana portions of the mixed oxides thereby leading to the formation of crystalline MVO_4 (M = In and La) surface compounds. In the case of V_2O_5/Ga_2O_3-TiO_2 sample, no such compound formation was observed, since the Ga^{3+} ionic radius (0.62 Å) is less than that of Ti^{4+}.

To understand the influence of various additives on the crystallite growth of titania, the crystallite size of anatase and rutile phases in various M_2O_3-TiO_2 (M = Ga, In and La) samples were estimated using the line broadening technique and shown in Table 1. The TiO_2 anatase (1 0 1) and rutile (1 1 0) reflections were used for crystallite size measurements in various samples. All M_2O_3–TiO_2 composite oxides in general retained anatase modification and its crystallite size increased with increasing calcination temperature. It is known that incorporation of an appropriate additive to TiO_2 retards the phase transformation of anatase to rutile and its crystallite size due to the formation of M–O–Ti bonds. In the present study, the degree of retardation varied from additive to additive. Specifically, the La_2O_3–TiO_2 composite oxide retained the smallest crystallites among other samples. The non-formation of TiO_2 (R) even up to 1073 K calcination is an interesting observation in the present study [6,17]. As shown in Table 1, the crystallite size of TiO_2 (A or R) in V_2O_5/M_2O_3-TiO_2 samples increased with increasing calcination temperature. The 773 K calcined samples retained anatase modification, whereas rutile dominates at higher calcinations (Table 1) in the case of V_2O_5/M_2O_3-TiO_2 samples (M = Ga and In). Retention of anatase modification up to 1073 K calcination, even in the presence of dispersed vanadia species in the case of V_2O_5/La_2O_3-TiO_2 sample, is an interesting observation from this study. It is a general phenomenon that the catalysts with smaller particle size exhibit better catalytic properties. In particular, the V_2O_5/Ga_2O_3-TiO_2 combination catalysts exhibited better catalytic properties for selective oxidation of 4-methylanisole to anisaldehyde [22].

The FTIR spectra of M_2O_3-TiO_2 and V_2O_5/M_2O_3-TiO_2 (M = Ga, In and La) samples calcined at various temperatures were recorded in the range of 400–4000 cm^{-1}. All supports in general exhibited strong absorption bands at 3400–3600 and 1625 cm^{-1}. Additionally, a new band at ∼650–830 cm^{-1} was also observed in the case of 1073 K calcined samples. The absorption bands between 3400 and 3600 cm^{-1} could be attributed to the presence of surface hydroxyl groups, which gradually decrease with increasing calcination temperature [41]. The band at 1625 cm^{-1}, due to the deformation vibrations of adsorbed water, was also gradually decreased after calcination at higher temperatures [42]. Anatase and rutile phases of titania exhibit strong absorption bands in the region of 850–650 and 800–650 cm^{-1}, respectively [43]. A gradual improvement in the region 850–650 cm^{-1} with increasing calcination temperature was noted suggesting that the titania is gradually transforming from an amorphous to a crystalline anatase phase in line with XRD observations. Further, there was no evidence for the presence of TiO_2 (R) phase in concurrence with the XRD analysis.

The FTIR spectra of various V_2O_5/M_2O_3-TiO_2 (M = Ga, In and La) catalysts calcined at different temperatures were recorded in the range 400–1800 cm^{-1}, where those bands due to $\nu_{V=O}$ are expected to be observed. Normally, the IR spectrum of pure crystalline V_2O_5 shows sharp absorption bands at 1020 and another at 820 cm^{-1} due to V=O stretching and V–O–V deformation modes, respectively [6]. The spectra of the various V_2O_5/M_2O_3-TiO_2 catalysts calcined at 773 K are mostly identical to those of pure supports. However, with increase in calcination temperature from 773 to 1073 K a gradual improvement in the absorption region between 670 and 540 cm^{-1} was observed indicating the formation of crystalline TiO_2 (A) phase. Additionally, two weak absorption bands were also observed at 960 and 910 cm^{-1}, which can be attributed to the presence of tetrahedral VO_x groups. This particular band in the range of 990–960 cm^{-1}, has been reported frequently for vanadia-titania catalysts having vanadium content close to the monolayer coverage [6]. Nakagawa et al. [44], reported that the V=O stretching frequency is

sensitive to the vanadium oxide loading and shifts from 1020 (pure V_2O_5) to 980 cm^{-1} thus indicating that vanadium oxide is present as an amorphous VO_x at low coverages, and both amorphous and crystalline V_2O_5 at high surface coverages. The disappearance of absorption band at 990–960 cm^{-1} was observed in the case of V_2O_5/M_2O_3-TiO_2 (M = In and La) samples at higher calcination temperatures. The formation of crystalline MVO_4 (M = In and La) phase may be the reason for the disappearance of the absorption band at 990–960 cm^{-1} of the dispersed VO_x species. Thus, FTIR measurements corroborate well with the XRD findings up to certain extent.

The samples of M_2O_3-TiO_2 and V_2O_5/M_2O_3-TiO_2 (M = Ga and La) calcined at different temperatures were investigated by XPS technique. The photoelectron peaks of O 1s, Ti 2p, Ga 3d and La 3d pertaining to the above samples are depicted in Figs. 3–6, respectively. Binding energies for O 1s, Ti 2p, Ga 3d, La 3d and V 2p core level peaks are shown in Table 2. All these figures and Table 2 clearly indicate that the XPS bands depend on calcination temperature and on the coverage of vanadium oxide on the support surface, in agreement with the earlier literature reports [45,46]. As presented in Fig. 3, the O 1s peak is, in general, broad and complicated due to non-equivalence of surface oxygen ions. The peak shape suggests that it is composed of more than one peak arising due to overlapping contributions of oxide ions

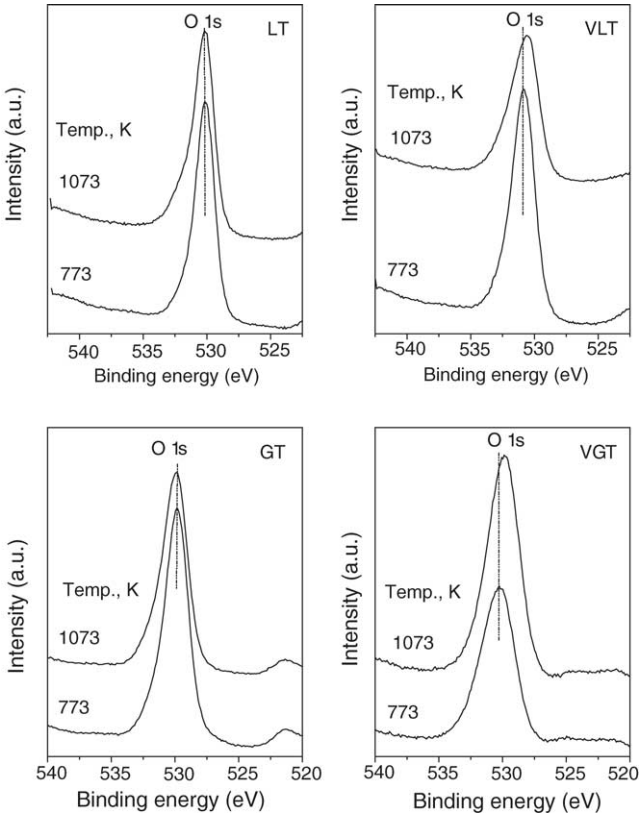

Fig. 3. O 1s XPS spectra of various M_2O_3-TiO_2 and V_2O_5/M_2O_3-TiO_2 (M = Ga^{3+} and La^{3+}) catalysts calcined at 773 and 1073 K temperatures.

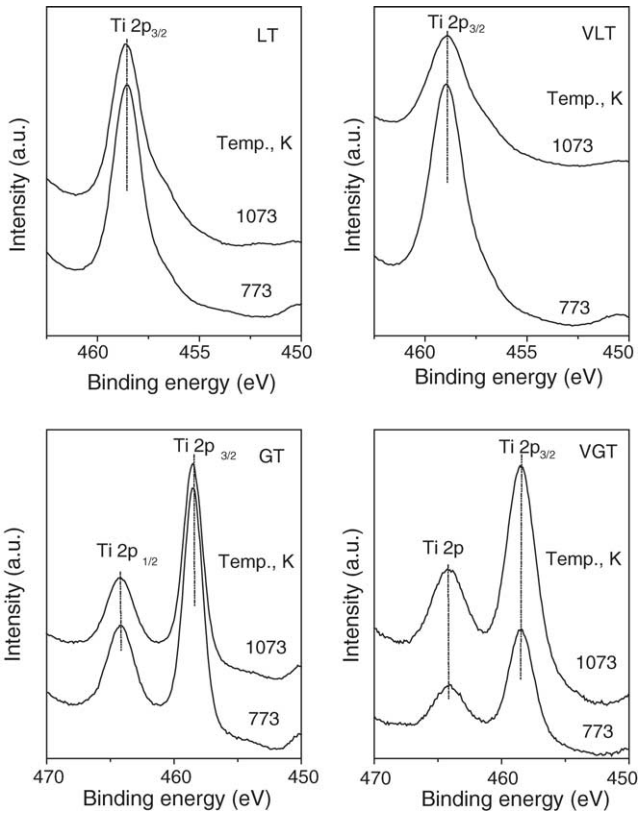

Fig. 4. Ti 2p XPS spectra of various M_2O_3-TiO_2 and V_2O_5/M_2O_3-TiO_2 (M = Ga^{3+} and La^{3+}) catalysts calcined at 773 and 1073 K temperatures.

from various components. The binding energy of the most intense O 1s peak (Table 2), in the case of Ga_2O_3-TiO_2 sample (Fig. 3), is almost constant with increasing calcination temperature. A slight shift towards higher binding energy and a clear broadening of the peak after impregnating with vanadia can be noted, due to strong interaction between the dispersed vanadia and titania portion of the composite oxide. Vanadia is known to accelerate the crystallization and transformation of anatase to rutile and also the formation of $V_xTi_{(1-x)}O_2$ rutile solid solution at higher calcination temperatures [6]. The increase in the intensity of the O 1s peak, in

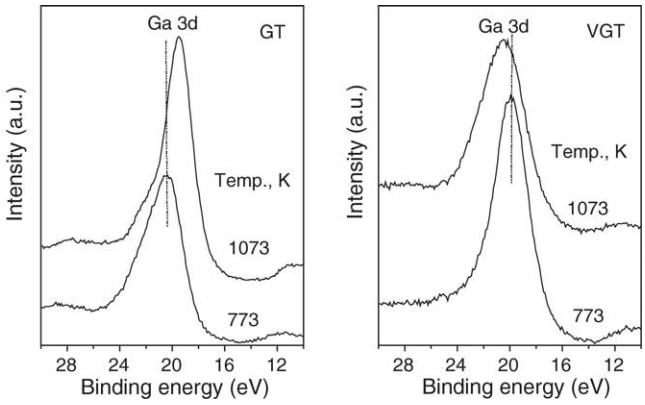

Fig. 5. Ga 3d XPS spectra of Ga_2O_3-TiO_2 and V_2O_5/Ga_2O_3-TiO_2 catalysts calcined at 773 and 1073 K temperatures.

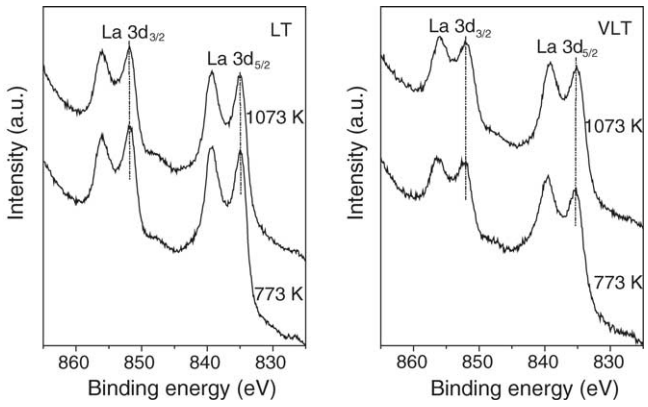

Fig. 6. La 3d XPS spectra of La_2O_3-TiO_2 and V_2O_5/La_2O_3-TiO_2 catalysts calcined at 773 and 1073 K temperatures.

the case of vanadia-impregnated samples could be attributed to the above reasons. Fig. 3 also represents the O 1s spectra of the La_2O_3–TiO_2 composite oxide, comprising of two distinct oxygen peaks. The intense peak at lower binding energy (530.1 eV) can be attributed to the oxide ions of titania and the one at higher binding energy (530.6 eV) belongs to lanthanum oxide ions, judging from the difference in the electronegativity of the elements involved and from literature [45,46]. The binding energy of the O 1s peak of pure composite oxide is constant, indicating no substantial change in the oxidation state of the elements involved. The O 1s spectra of the vanadia-impregnated samples are broad, which can be attributed to the selective interaction of the dispersed vanadium oxide with lanthana portion of the composite oxide leading to the formation of $LaVO_4$.

Table 2
Electron binding energy (eV) values of M_2O_3-TiO_2 and V_2O_5/M_2O_3-TiO_2 catalysts (M = Ga and La) calcined at different temperatures

Calcination temperature (K)	Binding energy (eV)			
	O 1s	Ti $2p_{3/2}$	Ga $3d_{5/2}$	V $2p_{3/2}$
Ga_2O_3-TiO_2				
773	529.9	458.5	20.4	–
873	529.8	458.5	20.0	–
973	529.9	458.5	19.7	–
1073	529.9	458.5	19.5	–
V_2O_5/Ga_2O_3-TiO_2				
773	530.2	458.5	19.9	517.3
873	530.1	458.5	20.0	517.1
973	530.0	458.5	20.2	517.0
1073	529.9	458.5	20.4	516.8
	O 1s	Ti $2p_{3/2}$	La $3d_{5/2}$	V $2p_{3/2}$
La_2O_3-TiO_2				
773	530.1	458.6	834.9	–
873	530.1	458.6	834.9	–
973	530.2	458.6	834.9	–
1073	530.2	458.6	834.9	–
V_2O_5/La_2O_3-TiO_2				
773	530.7	458.9	835.4	515.9
873	530.7	458.9	835.3	515.8
973	530.6	458.8	835.2	515.9
1073	530.6	458.8	835.2	516.0

Fig. 4 represents the Ti 2p photoelectron peaks of Ga_2O_3-TiO_2, V_2O_5/Ga_2O_3-TiO_2, La_2O_3-TiO_2 and V_2O_5/La_2O_3-TiO_2 samples. As observed from Table 2, the binding energy of the Ti $2p_{3/2}$ photoelectron peak ranged between 458.5 and 459.0 eV, which agree well with the values reported in the literature [20,45–47]. The intensity of the Ti 2p photoelectron peak of gallia-titania samples (Fig. 4) increased with increasing calcination temperature. The Ti $2p_{3/2}$ binding energy values are almost constant (458.5 eV) for all samples indicating that the Ti exists in +4 oxidation state. The intensity of the Ti 2p photoelectron peak of La_2O_3-TiO_2 samples (Fig. 4) decreased with increasing calcination temperature and the decrease being prominent in the case of vanadia containing samples. Redistribution of various component oxide species could be responsible for the observed decrease in the intensity of the Ti 2p peaks. The highly feasible acid–base interaction between vanadia and lanthana to form stable $LaVO_4$ compound leads to a total redistribution of the surface species thereby accounting for the substantial decrease in the intensity of the Ti 2p peak in the case of vanadia-impregnated samples.

The Ga 3d core level spectra of Ga_2O_3–TiO_2 composite oxide and the corresponding vanadia-impregnated sample calcined at different temperatures are shown in Fig. 5. As can be observed from Table 2, the Ga 3d binding energy for gallia-titania samples decreased and for vanadia containing samples increased with increasing calcination temperature. The decrease in the BE with increasing calcination temperature, in the case of pure support, could be attributed to partial reduction of gallia under the conditions of XPS analysis [48]. The corresponding increase in the intensity suggests that the crystallization of gallia is taking place at higher calcination temperatures in line with XRD observations. In the case of vanadia-impregnated samples, an increase in the binding energy and corresponding decrease in the intensity of Ga 3d peak could be attributed to surface segregation of gallia species under the influence of dispersed vanadia due to $V_xTi_{(1-x)}O_2$ rutile solid solution formation. Fig. 6 shows the La 3d spectra of La_2O_3-TiO_2 and V_2O_5/La_2O_3-TiO_2 samples calcined at different temperatures. The electron binding energy values observed at 834.9 and 851.8 eV, corresponding to La $3d_{5/2}$ and La $3d_{3/2}$, respectively, agree well with earlier literature reports [45,46,49]. In the case of La_2O_3-TiO_2 support, the intensity and binding energy of the La 3d line remained constant irrespective of calcination temperature, which indicates that the chemical state of lanthana is non-variant and corresponds to La(III) oxidation state. The increase in both intensity and binding energy of the La 3d XPS peaks observed in the case of vanadia containing samples are mainly due to the formation of $LaVO_4$ as observed at higher calcination temperatures from XRD measurements.

The V 2p XP spectra (not shown) of V_2O_5/Ga_2O_3-TiO_2 and V_2O_5/La_2O_3-TiO_2 samples were in general broad. The

broadening can be attributed to various factors including: (i) the presence of more than one type of V^{5+} with different chemical characteristics, which cannot be discerned by ESCA, and (ii) electron transfer between the active component and the support (metal oxide–support oxide interaction) [50–55]. The binding energy of the V 2p peak in the case of V_2O_5/Ga_2O_3-TiO_2 sample calcined at 773 K was observed to be 517.3 eV. With increasing calcination temperature from 773 to 1073 K the binding energy decreased from 517.3 to 516.8 eV. The decrease in binding energy with increasing calcination temperature indicates that some part of vanadium oxide is stablized in the lower oxidation (tetravalent) state. This may be due to the formation of $V_xTi_{(1-x)}O_2$ rutile solid solution between vanadia and titania, wherein the vanadium is in less than +5 oxidation state. The intensity of the V 2p spectra of V_2O_5/La_2O_3-TiO_2 samples increased with increasing calcination temperature. The V 2p BE values as presented in Table 2 indicate that vanadium is predominantly in V(V) oxidation state. The BE of the V $2p_{3/2}$ reported for V(V) oxidation state ranges between 517.4 and 516.4 eV [50–55]. The BE values as presented in Table 2 and an increase in the intensity with increasing calcination temperature also support the formation of $LaVO_4$ wherein both the constituent metals are in their highest oxidation state i.e. La(III) and V(V). Thus, the XPS results fairly support the conclusions drawn from XRD measurements.

2,6-Dimethylphenol is an important chemical intermediate in the polymer industry for engineering plastics [56]. The commercial synthetic method was based on a liquid phase process, where phenol is methylated with methanol using an alumina catalyst. However, this process not only requires high pressure and temperature, but also produces wide range of byproducts, including various isomers of xylenol [57]. Therefore, there are several advantages like continuous production, simplified product recovery, catalyst regenerability, etc. for carrying out this reaction in the vapor phase from cyclohexanone and methanol. Wang et al. [58] reported the synthesis of 2,6-dimethylphenol from methanol and cyclohexanone over vanadia-titania catalysts. However, the conversion and product selectivities reported are limited on this catalyst. Recently, mixed oxide supports have attracted much attention because of their better performance than their constituent single oxides for various reactions [21,59,60]. Therefore, this particular reaction was selected in the present investigation to study the catalytic properties of various M_2O_3-TiO_2 (M = Ga, In and La) composite oxides and their corresponding V_2O_5/M_2O_3-TiO_2 catalysts.

The activity and selectivity for the single step synthesis of 2,6-dimethyl phenol was investigated between 573 and 698 K. The activity and selectivity trends on various catalysts followed the same pattern with temperature. In general, an increase in the conversion with an increase in temperature was observed. The formation of some additional side products with traces of CO and CO_2 were also occasionally noted at higher temperatures. The change in conversion as a function of contact time at a fixed temperature of 673 K was also studied on various catalysts. A decrease in the conversion of cyclohexanone during the initial reaction period was observed for all the catalysts used, but stable activity was obtained within a few hours. The conversion and selectivity are calculated on cyclohexanone basis and almost all the excess methanol was recovered after the reaction. The conversion and selectivity results pertaining to synthesis of 2,6-dimethylphenol at 673 K temperature and normal atmospheric pressure over various samples prepared in the present study are shown in Table 3. An increase in the conversion of cyclohexanone was noted as the reaction temperature increases over all the catalysts studied in the present investigation. On all M_2O_3-TiO_2 (M = Ga, In and La) composite oxides, at low reaction temperatures the formation of 1-methoxycyclohexene, methyl formate, and dimethyl ether in large amounts was noted in addition to small amounts of 2-methylcyclohexanone, 2,6-dimethylcyclohexanone, and 2,6-dimethylphenol. When the reaction temperature was raised to 648 K and above, the selectivity towards 2-methylcyclohexanone and 2,6-dimethylcyclohexanone was more than the selectivity towards 2,6-dimethylphenol. However, at all these temperatures the formation of methyl formate, dimethyl ether, and CO_x in small quantities was also noted. In the case of V_2O_5/M_2O_3-TiO_2 catalysts, 2,6-dimethylphenol, 2,6-dimethylcyclohexanone, 2-methylcyclohexanone and 1-methoxycyclohexene were the main products. In general, the selectivity of 2,6-dimethylphenol increased with increasing reaction temperature and at the same time the selectivity towards 2,6-dimethylcyclohexanone, 2-methylcyclohexanone and 1-methoxycyclohexene were decreased drastically. The selectivity towards 2,6-dimethylphenol was high for all vanadia-impregnated samples when compared to that of pure support. The activity results suggest that 12 wt.% V_2O_5/La_2O_3-TiO_2 catalyst exhibits more 2,6-dimethylphenol yield (81%) and seem to be a promising catalyst for this reaction [61–65]. To the best of our knowledge, there are only a few reports in the open literature on the synthesis of 2,6-dimethylphenol from cyclohexanone and methanol in the vapour phase. In particular, Wang and Tsai investigated the synthesis of 2,6-dimethylphenol from methanol and cyclohexanol or a mixture of cyclohexanol and cyclohexanone (KA-oil) over a Cr/MgO catalyst and reported about 54% yield at 673 K

Table 3
Activity and Selectivity results pertaining to the synthesis of 2,6-dimethylphenol (2,6-DMP) from methanol and cyclohexanol mixture over various M_2O_3-TiO_2 and V_2O_5/M_2O_3-TiO_2 catalysts (M = Ga, In and La) at 673 K and under normal atmospheric pressure

Catalyst	Conversion (%)	2,6-DMP selectivity (%)	2,6-DMP yield
Ga_2O_3-TiO_2	91	28	25
In_2O_3-TiO_2	64	19	12
La_2O_3-TiO_2	91	28	25
V_2O_5/Ga_2O_3-TiO_2	90	65	59
V_2O_5/In_2O_3-TiO_2	88	66	58
V_2O_5/La_2O_3-TiO_2	96	84	81

[62–64]. A slight improvement in the activity of Cr/MgO catalyst was also noted up on addition of Pt promoter to Cr/MgO catalyst [65]. The better activity of 12 wt.% V_2O_5/La_2O_3-TiO_2 catalyst in the present study could be due to various factors such as a reasonably high specific surface area of the sample, a reasonably large quantity of V_2O_5 in a highly dispersed state, and combined acid–base and redox properties together in this complex catalyst system. However, further studies are required to understand the nature and surface structure of these catalysts and their potential application. Of course, the formation of 2,6-dimethylphenol from methanol and cyclohexanone is a complex reaction and proceeds in a different manner from that of normal methylation of aromatic compounds [21,66].

As envisaged earlier, in the first step of reaction the cyclohexene condenses with a methanol molecule, in its another isomeric form enol, and produces 1-methoxycyclohexene, which is observed as one of the side products [21]. Thus, formed 1-methoxycyclohexene over isomerization produces 2-methylcyclohexanone. The so formed 2-methylcyclohexanone by condensing with another molecule of methanol produces 2,6-dimethylcyclohexanone. The formed 2,6-dimethylcyclohexanone by oxidative dehydrogenation probably produces 2,6-dimethylphenol. However, detailed studies are highly essential to establish the mechanism of this complex reaction. It is an established fact in the literature that transition metal oxides, such as V_2O_5, MoO_3, etc., are very active for the oxidative dehydrogenation of organic molecules [35,67]. The mixed oxide supports when impregnated with a redox metal oxide are expected to show better catalytic properties [21,35,68]. Recently, Deo and Wachs [69] investigated methanol oxidation on a number of supported vanadium oxide catalysts. They found that the activity of the alcohol oxidation correlates with the extent of reduction and strength of V=O and V–O–M bonds. However, it is difficult to establish such a direct correlation in the present study because of the complexity of the reaction mechanism.

4. Conclusions

The following conclusions can be drawn from the present study. (i) All M_2O_3-TiO_2 (M = Ga, In and La) binary oxides reported in the present study are interesting supports for the dispersion of vanadium oxide. (ii) The co-precipitated M_2O_3-TiO_2 mixed oxides when calcined at 773 K are in X-ray amorphous state and exhibit reasonably high specific surface area. (iii) The M_2O_3-TiO_2 mixed oxides also accommodate a monolayer equivalent of (12 wt.%) V_2O_5 in a highly dispersed state on their surface. Further, the V_2O_5/M_2O_3-TiO_2 catalysts are also thermally stable up to 873 K calcination temperature. The dispersed V_2O_5 selectively interacts with M_2O_3 portion of the M_2O_3-TiO_2 mixed oxides and readily forms MVO_4 (M = In and La) compound with the liberation of TiO_2 when subjected to thermal treatments beyond 873 K. The liberated TiO_2 appears in the form of anatase as well as rutile phases. (iv) Interestingly, the 12% V_2O_5/La_2O_3-TiO_2 mixed oxide catalyst exhibits better catalytic properties for the vapour phase synthesis of 2,6-dimethylphenol from methanol and cyclohexanone mixtures. A high activity of this catalyst could be related to more quantity of V_2O_5 in a highly dispersed state apart from acid–base and redox properties of the catalyst. Further studies are essential to understand the mechanism of this reaction and commercial viability of these catalysts.

Acknowledgments

Ataullah Khan thanks Department of Science and Technology, New Delhi for a Junior Research Fellowship under SERC Scheme (SP/S1/H-20/98).

References

[1] J. Whitehead, Titanium compounds, inorganic, in: M. Grayson (Ed.), Kirk-Othmer Encyclopaedia of Chemical Technology, third ed., vol. 23, Wiley, New York, 1983, p. 131.
[2] K.I. Hadjiivanov, D.G. Klissurski, Chem. Soc. Rev. 25 (1996) 61, and references therein.
[3] M. Wagemaker, G.J. Kearley, A.A. van Well, H. Mutka, F.M. Mulder, J. Am. Chem. Soc. 125 (2003) 840.
[4] J.C. Vedrine (Ed.), Eurocat oxide, Catal. Today, vol. 20, 1994, p. 1, and references therein.
[5] H. Bosh, F. Janssen, Catal. Today 2 (1988) 369.
[6] G.C. Bond, S.F. Tahir, Appl. Catal. 71 (1991) 1, and references therein.
[7] G. Deo, I.E. Wachs, J. Haber, Crit. Rev. Surf. Chem. 4 (1994) 141, and references therein.
[8] M.R. Hoffmann, S.T. Martin, W. Choi, D.W. Bahnenann, Chem. Rev. 69 (1995) 95.
[9] M. Apno, Res. Chem. Intermed. 11 (1989) 67.
[10] M. Taramasso, G. Perego, B. Notari, U.S. Patent 4, 410, 501 (1983).
[11] M.A. Vannice, R.L. Garten, J. Catal. 56 (1979) 236.
[12] K. Arata, K. Tanabe, Chem. Lett. 1017 (1979).
[13] A. Baiker, P. Dollenmeier, M. Glinski, A. Reller, Appl. Catal. 35 (1987) 351.
[14] H.M. Matralis, M. Ciardelli, M. Ruwet, P. Grange, J. Catal. 157 (1995) 368.
[15] R. Kozlowski, R.F. Pettifer, J.M. Thomas, J. Phys. Chem. 87 (1983) 5176.
[16] F. Roozeboom, M.C. Mittlemeijer-Hazeleger, J.A. Moulin, J. Medema, V.H.J. de Beer, P.J. Gellings, J. Phys. Chem. 84 (1980) 2783.
[17] S.R. Yoganarasimhan, C.N.R. Rao, Trans. Faraday Soc. 58 (1962) 1579.
[18] K.-N.P. Kumar, Appl. Catal. A: Gen. 119 (1994) 163.
[19] B.M. Reddy, B. Manohar, S. Mehdi, J. Solid State Chem. 97 (1992) 317.
[20] B.M. Reddy, I. Ganesh, E.P. Reddy, J. Phys. Chem. B 101 (1997) 1769.
[21] B.M. Reddy, I. Ganesh, J. Mol. Catal. A: Chem. 169 (2001) 207.
[22] B.M. Reddy, I. Ganesh, E.P. Reddy, A. Fernández, P.G. Smirniotis, J. Phys. Chem. B 105 (2001) 6227.
[23] B.M. Reddy, P.M. Sreekanth, E.P. Reddy, Y. Yamada, Q. Xu, T. Kobayashi, J. Phys. Chem. B 106 (2002) 5695.
[24] B.M. Reddy, A. Khan, Y. Yamada, T. Kobayashi, S. Loridant, J.C. Volta, J. Phys. Chem. B 107 (2003) 5162.

[25] J.R. Mowry, R.F. Anderson, J.A. Jonson, J. Oil Gas (1985) 128.
[26] S.N. Burford, E.E. Davis, U.S. Patent 41,573,565 (1979).
[27] M. Ogura, M. Hayashi, E. Kikuchi, Catal. Today 45 (1998) 139.
[28] C.A. Le Duc, J.M. Campbell, J.A. Rossin, Ind. Eng. Chem. Res. 35 (1996) 2473.
[29] G.S. Lane, Z. Kalenik, E.E. Wolf, Appl. Catal. 53 (1989) 183.
[30] H. Borchert, M. Baerns, J. Catal. 168 (1997) 315.
[31] K.N.P. Kumar, K. Keizer, A.J. Burggraaf, J. Mater. Chem. 3 (1993) 1412.
[32] U. Trudinger, G. Muller, K.K. Unger, J. Chromatogr. 35 (1990) 111.
[33] H.P. Klug, L.E. Alexander, X-ray Diffraction Procedures for Polycrystalline and Amorphous Materials, second ed., Wiley, New York, 1974.
[34] B.M. Reddy, M.V. Kumar, K.J. Ratanam, Appl. Catal. A: Gen. 181 (1999) 77.
[35] B.M. Reddy, I. Ganesh, B. Chowdhury, Catal. Today 49 (1999) 115.
[36] I.A. Rozdin, F.M. Spiridonov, M.N. Sotnikova, L.N. Komissarovo, V.E. Plyushchev, Neorg. Mater. 10 (1971) 1801.
[37] I.A. Rozdin, S.S. Plotkin, V.E. Plyushchev, N.I. Sorokin, Neorg. Mater. 11 (1975) 178.
[38] R. Gopalan, Y.S. Lin, Ind. Eng. Chem. Res. 34 (1995) 1189.
[39] J. Lin, J.C. Yu, J. Photochem. Photobiol. A: Chem. 116 (1998) 63.
[40] C. Anderson, A.J. Bard, J. Phys. Chem. 98 (1994) 1769.
[41] H.H. Kung, Transition metal oxides, surface chemistry and catalysis, Stud. Surf. Sci. Catal. 45 (1988) 57.
[42] A. Jentys, G. Warecka, M. Derewinski, J.A. Lercher, J. Phys. Chem. 93 (1989) 4837.
[43] R.A. Nyquist, L.L. Putzig, M.A. Leugers, Handbook of Infrared and Raman Spectra of Inorganic Compounds and Organic Salts, Academic Press, 1997.
[44] Y. Nakagawa, J. Ono, H. Miyata, Y. Kubokawa, J. Chem. Soc., Faraday Trans. 79 (1983) 2929.
[45] Practical surface analysis, in: D. Briggs, M.P. Seah (Eds.), Auger and X-ray Photoelectron Spectroscopy, vol. 1, second ed., Wiley, New York, 1990.
[46] C.D. Wagner, W.M. Riggs, L.E. Davis, J.F. Moulder, Handbook of X-ray Photoelectron Spectroscopy, Perkin-Elmer Corporation, Minnesota, 1978.
[47] G.A. Sawatzky, D. Post, Phys. Rev. B20 (1979) 1546.
[48] H. Iwakuro, C. Tatsuyama, S. Ichimura, Jpn. J. Appl. Phys. 21 (1982) 94.
[49] L.P. Haack, C.R. Peters, J.E. deVries, K. Otto, Appl. Catal. A: Gen. 87 (1992) 103.
[50] W.P. Griffith, P.J.B. Lesniak, J. Chem. Soc. A (1969) 1066.
[51] H. Knözinger, G. Mestl, Top. Catal. 8 (1999) 45.
[52] I.E. Wachs, Top. Catal. 8 (1999) 57.
[53] I. Imamura, S. Ishida, H. Taramoto, Y. Saito, J. Chem. Soc. Faraday Trans. 89 (1993) 757.
[54] N.K. Nag, F.E. Massoth, J. Catal. 124 (1990) 127.
[55] V.I. Bukhtiyarov, Catal. Today 56 (2000) 403.
[56] J.M. Margolis, Engineering Thermoplastics: Properties and Applications, Dekker, New York, 1985.
[57] K. Weissermel, H.-J. Arpe, Industrielle Organische Chemie, Verlag Chemie, GmbH, Weium, Germany, 1976.
[58] F.L. Wang, L. Yu, W.S. Lee, W.F. Wang, J. Chem. Soc. Chem. Commun. (1994) 811.
[59] I. Wang, R.C. Chang, J. Catal. 107 (1987) 195.
[60] B.E. Hand, M. Maciejewski, A. Baiker, J. Catal. 134 (1992) 75.
[61] I. Ganesh, Ph.D. Thesis, Osmania University, India, 1999.
[62] F.L. Wang, T.F. Tsai, Appl. Catal. A: Gen. 201 (2000) 91.
[63] F.L. Wang, T.F. Tsai, Y.H. Tsai, Y.K. Cheng, Catal. Appl. A: Gen. 126 (1995) L229.
[64] F.L. Wang, T.F. Tsai, Catal. Today 44 (1998) 259.
[65] F.L. Wang, T.F. Tsai, J. Chin. Chem. Soc. 47 (2000) 163.
[66] G.S. Devi, G. Giridhar, B.M. Reddy, J. Mol. Catal. A: Chem. 181 (2002) 173.
[67] A. Lisovski, C. Ahroni, Catal. Rev. Sci. Eng. 36 (1994) 25.
[68] B.M. Reddy, I. Ganesh, B. Chowdhury, Chem. Lett. (1997) 1145.
[69] G. Deo, I.E. Wachs, J. Catal. 156 (1994) 323.